Quaternary International 442 (2017) 35–49

Contents lists available at ScienceDirect

Quaternary International

journal homepage: www.elsevier.com/locate/quaint

Relative sea-level changes during the Holocene in the Río de la Plata, Argentina and Uruguay: A review

Aldo R. Prieto [a,*], Dominique Mourelle [a], W. Richard Peltier [b], Rosemarie Drummond [b], Isabel Vilanova [c], Lila Ricci [d]

[a] Instituto de Investigaciones Marinas y Costeras, CONICET, Universidad Nacional de Mar del Plata, Funes 3250, B7602AYL Mar del Plata, Argentina
[b] Department of Physics, University of Toronto, M5S 1A7 Toronto, ON, Canada
[c] CONICET, Museo Argentino de Ciencias Naturales "Bernardino Rivadavia", Avda. Ángel Gallardo 470, C1405DJR Buenos Aires, Argentina
[d] Departamento de Matemática, Universidad Nacional de Mar del Plata, Funes 3250, B7602AYL Mar del Plata, Argentina

ARTICLE INFO

Article history:
Available online 10 March 2016

Keywords:
Río de la Plata
Sea-level changes
Holocene
Argentina
Uruguay
GIA models

ABSTRACT

This study critically reviews the relative sea-level (RSL) data from the Río de la Plata (RDP) (Argentina and Uruguay) in order to analyze the Holocene RSL changes in this region and thus capture the general trend illustrated by both the data and the high-degree polynomial regression analyses which show good agreement with the ICE-6G_C (VM6) model. The previously inferred Holocene sea-level histories reconstructed from palynological and diatom records from the northern and the southern RDP are also compared to the RSL curves proposed in this work. Analysis of the RSL database revealed that the RSL rose to reach the present level at or before c. 7000 cal yr BP, with the peak of the sea-level highstand c. +4 m between c. 6000 and 5500 cal yr BP (depending on the statistical method used) or at c. 7000 cal yr BP according to the ICE-6G model prediction, gradually falling after this time to the present position. The subaerial data tell a consistent story for the last 6000 years for the RDP but the subsurface data are not in agreement with these data or with the glacial isostatic adjustment (GIA) predictions. Since much of the subaerial data come from shells on beaches, beach ridges and storm beaches, they cannot be strictly interpreted as RSL index points. It seems likely that the predicted curves are somewhat high and could be overestimated. The "smooth" model of the late Holocene sea-level decline is in close agreement with both the GIA model predictions and the reconstruction of RSL from palynological and diatom records. The models provide no evidence to suggest that there has been a significant trend of change in the speed of sea-level fall or oscillations during the falling stage system tract. The non-parametric regression model, the GIA predictions and the trend inferred by palynological and diatom data trace out a slow sea-level fall for the last c. 6000 cal yr BP. We critically assessed published Holocene sea-level data from the RDP to produce a Holocene RSL curve of sufficient quality to provide a location in this area for testing theoretical models for the Atlantic coast of South America.

1. Introduction

Several sea-level reconstructions are available from the region on the border between Argentina and Uruguay (28° to 38° S; Fig. 1) along the east coast of the South American continent. Holocene sea-level history has been reconstructed for different areas of Buenos Aires province (e.g. Isla, 1989; Aguirre and Whatley, 1995; Cavallotto et al., 1995; Gómez and Perillo, 1995; Isla and Espinosa, 1998; Gómez et al., 2006) and Uruguay (Bracco et al., 2011, 2014; Martínez and Rojas, 2013, 2014). With the exception of the work by Gómez et al. (2006) and Bracco et al. (2011) who have indicated a negative relative sea-level (RSL) oscillation around 2650 ^{14}C yr BP in Bahía Blanca estuary (Fig. 1) and a negative short-term oscillation at c. 4500 cal yr BP for the Uruguayan coast (Fig. 2) respectively, other publications have proposed a simple regressive trend to the present position after the emplacement of a maximum Holocene highstand. In works in which RSL curves have been proposed, these have been constructed using a simple qualitative approach, with the exception of the work by Martínez and Rojas (2013) in which a non-parametric smoothing technique was employed. However, the

* Corresponding author.
E-mail addresses: aprieto@mdp.edu.ar (A.R. Prieto), domodica@gmail.com (D. Mourelle), peltier@atmosp.physics.utoronto.ca (W.R. Peltier), ivilanova@macn.gov.ar (I. Vilanova), lricci@mdp.edu.ar (L. Ricci).

http://dx.doi.org/10.1016/j.quaint.2016.02.044
1040-6182/

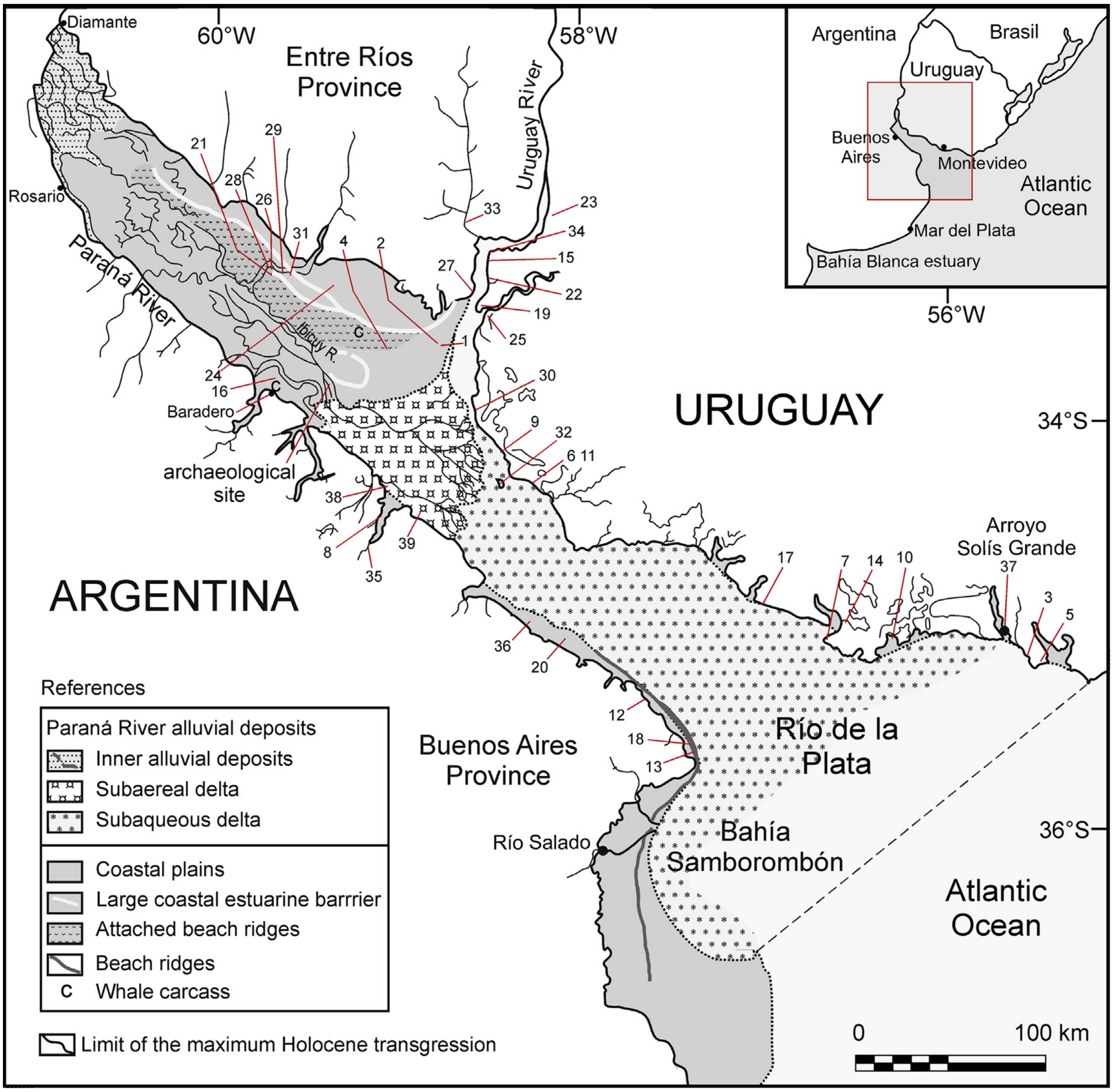

Fig. 1. Location map showing the Rio de la Plata and the sites from index points where obtained (Table 1). Regional geomorphologic map modified from Cavallotto (2002) and Colombo et al. (2014).

timing and amplitude of the mid-Holocene highstand and regressive trend of the RSL on the border between Argentina and Uruguay are not well resolved, partly because of the varied RSL reconstruction methods used and also because the data used in the reconstruction of the curves came from different environments. The only evidence of late Pleistocene sea-level variation for the Argentine Shelf is that provided by Guilderson et al. (2000). However there is some question as to whether their data is actually indicative of sea-level at all.

Particularly for the Río de la Plata (RDP), a Holocene RSL curve was presented by Cavallotto et al. (2004) based on 14 uncalibrated ^{14}C ages from selected samples from the southwestern coast of the RDP (Argentina). This RSL curve was re-plotted by Gyllencreutz et al. (2010) using the same index points and qualitative approach but using the calibrated ages. It shows rising sea-levels following the Last Glacial Termination (LGT), reaching a RSL maximum of +6.5 m above present at c. 6500 cal yr BP, followed by a stepped regressive trend towards the present (Fig. 2a). On the other hand, Holocene RSL curves for the Uruguayan coast that include data from both the northeastern RDP and the Atlantic coast have been reconstructed by Bracco et al. (2011, 2014) and Martínez and Rojas (2013, 2014). These curves show some discrepancies concerning the timing and magnitude of the mid-Holocene highstand and the regressive trend (Fig. 2b). However, none of these authors have taken into account the fact that the RDP history might have been different from the Uruguayan oceanic coast during the Holocene. They rather served to revive the controversy between smooth (linear) and oscillating mid- and late-Holocene sea-level curves for southern South America (e.g. Angulo et al., 2006; Gómez et al., 2006).

Rostami et al. (2000) demonstrated that RSL predictions to the north of 36°S in the Atlantic Ocean of South America based upon the ICE-4G (VM2) deglaciation model, are reasonably well predicted by the theory. However, Milne et al. (2005) suggested that the data considered for sea-level predictions were of relatively poor quality and for that reason they did not use them in constraining their models for South America. We will argue herein that the data for this region are actually of rather high quality.

As significant differences exist in the interpretations of the sea-level curves from the RDP (Argentina and Uruguay), we decided to use a compilation of published data to achieve the following aims: (1) to critically review the data in order to test whether smooth or stepped sea-level curve trends from regression time–elevation plots best characterized the data; (2) to compare with the predictions of the best available glacial isostatic adjustment (GIA) model to better understand the distinct spatial trends evident in the data; and (3) to discuss changes in sea-level during the Holocene. RSL curves are proposed and discussed from compiled data from Holocene estuarine-marine molluscs collected in the littoral zone from both coasts and from the inner part and the subsurface of the RDP. The inferred Holocene sea-level histories reconstructed from palynological and diatom records from the northern (Arroyo Solís Grande; Mourelle et al., 2015) and the multi-proxy record from the southern RDP (Río Salado; Vilanova and Prieto, 2012) are also compared to the RSL curves proposed in this work.

2. Regional setting

The RDP (Fig. 1) constitutes the final outlet of La Plata Drainage Basin, the second largest river system in South America, covering an area of approximately 3.2×10^6 km^2 (Acha et al., 2008). The RDP is formed by the confluence of the Paraná and Uruguay rivers and is approximately 290 km long, widening from ~40 km at the upper reaches to 220 km at its outlet into the Atlantic Ocean (Pousa et al., 2013). The estuary is characterized by a salt-wedge regime; low seasonality in the river discharge; low tidal amplitude (modern astronomical mean tide is ~0.90 m); a broad and permanent connection to the sea; and high susceptibility to atmospheric forcing due to shallowness and its increasing downstream width (Acha et al., 2008). Tidal amplitude varies across the estuary with greater values along the Argentinean coast (amplitude 1 m) than along the Uruguayan coast (amplitude 0.3 m) and can be strongly modified by meteorological events (Sepúlveda et al., 2004). The higher level registered at the coast of Buenos Aires was 3.90 m over the mean sea-level in April 15, 1940. The maximum height above mean sea-level recorded in the gauge station of Montevideo was 4.7 m above sea-level during a storm on July 10, 1923 (Martínez and Rojas, 2013). Freshwater runoff is not an important contributing factor in estimating extreme levels in the region since flooding events are mainly due to a combination of tides and storm surge (D'Onofrio et al., 2008). The estuary is often swept by positive and negative storm surges due to strong southeasterly and northwesterly winds, respectively (D'Onofrio et al., 2008). Southeasterly winds push the RDP waters upriver, causing severe flooding. This frequent phenomenon, locally known as “sudestada”, is characterized by a gradual increase in the SE-SSE wind velocity accompanied by persistent rainfall (Servicio de Hidrografía Naval, 1999). The changes in frequency and duration of positive surge increase the probability of flooding of coastal areas. When the RDP is higher than about 2.80 m these areas are severely affected and they are completely flooded when the water level reaches 3.50 m (D'Onofrio et al., 2008). The increasing trend in the mean sea-level in the context of the global warming process may lead to a rise of as much as 1 m during the present century. Under such conditions all the areas of metropolitan Buenos Aires that are below 5 m above mean sea-level would be potentially threatened by extraordinary storms (D'Onofrio et al., 2008).

From the geomorphological point of view, the term “Río de la Plata” corresponds to a set of genetically interrelated landforms comprising both the subaerial and the subaquatic delta as well as the coastal plains of the northeastern Buenos Aires Province and southern Entre Ríos Province of Argentina, and reduced estuarine areas of southwestern Uruguay (Fig. 1) (Cavallotto et al., 1999).

A very distinctive feature of the inner RDP is the fact that the composite coastal estuarine barrier extends for approximately 220 km from the western shores of the Uruguay River westward along the left margin of the inner RDP (Colombo et al., 2014) (Fig. 1) and a complex beach consisting of an extensive strandplain composed of a number of attached beach ridge sets exists which formed subsequent to mid-Holocene time (Cavallotto et al., 2005; Colombo et al., 2014) (Fig. 1). These beach ridges are generally composed of well-sorted, fine-grained siliciclastic sand (Colombo et al., 2014). Some shell-dominated accumulations of *Erodona mactroides* are locally important (Cavallotto et al., 2005). The right margin of RDP is occupied by the remnants of beach ridges, tidal flats, small estuaries of minor streams and alluvial plain from the northeastern of Buenos Aires province and south of Entre Ríos province and the present delta of the Paraná River (Cavallotto et al., 2002; Colombo et al., 2014) (Fig. 1). The left margin is occupied by reduced estuarine areas (Cavallotto et al., 1999) where marshes partially sealed by dunes are formed at the lower reaches of major rivers that flow into the RDP (Fig. 1). They receive the overflow water from RDP when the flow exceeds the drainage capacity of the narrow channel mouths during spring high tides, and are thus intermittently flooded (MTOP, 1980), producing a salinity gradient in the marshes within the riverine estuary. Because of the presence of shallow lakes and marshes, much of the solid materials carried by major streams do not reach the RDP. These act as sediment traps limiting the sediment supply to the coastal zone.

3. Materials and methods

3.1. Data set

Our compilation contains more than 80 radiocarbon dates already published for the RDP. Prior to performing the necessary analyses, we checked carefully for data quality and limitations, so that those having contradictory or unclear information about location, altitude, the material dated, ages, and laboratory references were excluded. Moreover, we restricted the selected paleo-sea-level data set to data obtained subsequent to 1980 because the older radiocarbon data had high standard deviations. We also excluded all those samples for which the literature suggested there to be evidence that the material dated was subject to reworking, as well as those obtained from archaeological deposits. We have considered for our analyses mainly estuarine-marine mollusks dated with ^{14}C (AMS or conventional) obtained from mainly beach–ridge and beach storm deposits, which contain well preserved shells as published by the authors of each examined paper. This required an extensive search of more than 30 articles and technical reports where radiocarbon dates were originally published and first described. Contact with authors or dating laboratories was also established in several instances to verify their records. Therefore, the descriptions of some of the original data has been completed (lab number, dated material) or corrected (coordinates, age error), and may thus differ from that contained in the initially published records. On the basis of this “culling” of the original data set we have limited our analysis to 56 index points, of which 66% corresponds to the estuarine mollusk *E. mactroides* from 39 different sites along both coasts of the RDP (Fig. 1, Table 1). The co-ordinates of the index points from Argentina are referred to the present mean water level at the Mar del Plata tide-gauge. The co-ordinates of the Uruguayan index points are referred to the “official zero” for Uruguay. To make the sea-level heights comparable, 0.217 m was subtracted from the values of the heights above sea-level of Uruguay index points (SIRGAS Project, 1997). The vertical uncertainty with respect to the mean sea-level for beach ridge and beach storm deposits results from the present-day tidal range of 1 m, which was determined at the tide-gauge of the Port of Buenos Aires.

Table 1
Radiocarbon-dated sea-level data from Río de la Plata from previous publications calibrated in this study. C.: Country: Ar: Argentina; Uy: Uruguay. Ecological data: F: freshwater, B: brackish, O: open marine (Codignotto and Aguirre, 1993).

Sites	C.	Name	Latitude	Longitude	Lab. code	^{14}C age (yr BP)		Calibrated age range (cal. yr BP)			Material dated	Salinity	Elevation (m)		MSL error +/− (m)	Depositional environment	Reference	MA
						Age	Error +/−	Max	Median	min			MSL	Error +/−				
1	Ar	Entre Ríos	33°31′00.70″	58°39′36.30″	UIC10499	1770	41	1723	1644	1542	*Neocorbicula paranensi*	B/F	1.8		1	Plain beaches	Cavallotto et al. (2002, 2005)	A
2	Ar	Entre Ríos	33°29′59.00″	58°40′24.60″	UIC10500	1902	41	1891	1795	1707	*Neocorbicula limosa*	B/F	2		1	Plain beaches	Cavallotto et al. (2002, 2005)	B
3	Uy	Punta Fría	34°53′20.00″	55°16′37.00″	LP-817	2490	70	2313	2141	1956	*Tegula patagonica*	O	1.8		1	Parautochthonous shell concentrations in sand	Martínez et al. (2006); Rojas and Urteaga (2011); S. Martínez (pers. com., 2013)	C
4	Ar	Entre Ríos	33°31′33.20″	58°55′55.90″	UIC10498	2530	35	2304	2198	2084	*Erodona mactroides*	B	2.5		1	Plain beaches	Cavallotto et al. (2002, 2005)	
5	Uy	Punta Rasa	34°53′57.00″	55°13′51.00″	AA93720	2875	86.7	2789	2608	2350	*Glycymeris longior*	O	1.8		1	Beach storm	Rojas and Urteaga (2011); Martínez and Rojas (2013)	D
6	Uy	Punta Pereira	34°12′23.96″	58°4′8.49″	LP-753	3300	60	3313	3126	2950	*Erodona mactroides*	B	2.8		1	Parautochthonous shell concentrations in sand	Martínez et al. (2006)	E
	Uy	Punta Pereira	34°12′24.00″	58°4′8.00″	LP-775	3590	62.4	3635	3478	3329	*Erodona mactroides*	B	1.8		1	Parautochthonous shell concentrations in sand	Martínez et al. (2006); S. Martínez (pers. com., 2013)	E
7	Uy	Punta Espinillo	34°50′16.00″	6°25′23.00″	AA83199	3501	40	3485	3377	3245	*Notocochlis isabelleana*	O	1.5	0.25	1	Beach storm	Rojas and Urteaga (2011); Martínez and Rojas (2013)	D
8	Ar	Barrio Santa Brígida (Río Luján)	34°18′31.25″	58°54′13.39″	LP-1347	3640	70	3715	3534	3357	*Erodona mactroides*	B	3		1	Estuarine	Fucks and De Francesco (2003)	
9	Uy	Carmelo	34°2′38.00″	58°15′37.00″	LP-1375	3710	60	3803	3621	3459	*Erodona mactroides*	B	1.5	0.25	1	Fragmented shells in sharp sand with gravel	Rojas (2002); Martínez and Rojas (2013)	
10	Uy	Montevideo	34°52′39.16″	56°1′18.67″	URU0009	3790	190	4243	3736	3252	*Ostrea* sp.	O	2.8	0.50	1	Beach	Boksar and Pantazi (1998)	
11	Uy	Conchillas	34°12′26.17″	58°4′10.44″	URU0077	3830	52.8	3924	3770	3612	*Erodona mactroides*	B	2.8	0.25	1	Beach	Boksar and Pantazi (1998)	
12	Ar	Punta Atalaya	35°8′30.00″	57°23′55.00″	LP-351	4130	90	4419	4181	3914	*Mactra isabelleana*	B	5		1	Beach ridge	Cavallotto et al. (2004); J.L. Cavallotto (pers. com., 2013)	
13	Ar	Punta Piedras	35°23′52.00″	57°09′00.00″	LP-200	4380	60	4770	4521	4358	*Noetia bisulcata*	O	5		1	Beach ridge	Cavallotto et al. (2004); J.L. Cavallotto (pers. com., 2013)	
14	Uy	Parque Lecoq	34°47′11.00″	56°19′50.00″	AA93721	4481	41.6	4799	4666	4523	*Ostreola equestris*	O	2.8		1	Beach storm	Martínez and Rojas (2013); S. Martínez (pers. com., 2013)	
15	Uy	Las Cañas	33°9′43.00″	58°21′36.00″	LP-913	4550	62.4	4878	4735	4532	*Erodona mactroides*	B	3.8		1	Parautochthonous shell concentrations in sand	Martínez et al. (2006)	
16	Ar	Baradero	33°50′	59°30′	LP-1818	4720	70	5209	4958	4806	*Erodona mactroides*	B	1.15		1	Estuarine	Fucks et al. (2011)	

17	Uy	Arroyo Mauricio	34°42′30.20″	56°41′39.66″	URU0159	4750	70	5230	4999	4828	*Tagelus* sp.	B	4.8		1	Levee	Boksar and Pantazi (1998)	
18	Ar	Canal San Felipe	35°22′41.00″	57°09′54.00″	LP-568	4930	100	5490	5234	4937	*Noetia* sp.	O	4.2		1	Beach ridge	Colado et al. (1995)	F
	Ar	Canal San Felipe	35°22′41.00″	57°09′54.00″	LP-577	5120	70	5597	5471	5301	*Mactra* sp. + *Noetia* sp.+ unidentified shells	B/O	4.4		1	Beach ridge	Colado et al. (1995)	
19	Uy	Tabaré	33°21′41.00″	58°21′6.00″	LP-1372	4930	70	5445	5243	5022	*Erodona mactroides*	B	3.5	0.25	1	Backshore	Rojas (2002); Martínez and Rojas (2013)	
20	Ar	Estancia Bibiloni	34°56′50.00″	57°50′0.00″	LP-313	5150	70	5631	5500	5315	*Pachycymbiola brasiliana*	O	4.9		1	Beach ridge	Cortelezzi et al. (1992)	
21	Ar	Estancia La Calera 1	33°25′12.00″	58°34′48.00″	AC-0127	5280	100	5883	5642	5435	*Erodona mactroides*	B	4.2	0.50	1	Beach ridge	Albero and Angiolini (1983)	G
	Ar	Estancia La Calera 2	33°25′12.00″	58°34′48.00″	AC-0126	5410	110	6035	5774	5548	*Erodona mactroides*	B	4.5	0.50	1	Beach ridge	Albero and Angiolini (1983)	
	Ar	Estancia La Calera 3	33°25′12.00″	58°34′48.00″	AC-0128	5490	110	6125	5858	5605	*Erodona mactroides*	B	3.7	0.50	1	Beach ridge	Albero and Angiolini (1983)	
	Ar	Estancia La Calera 4	33°25′12.00″	58°34′48.00″	AC-0129	5530	110	6172	5908	5651	*Erodona mactroides*	B	3.3	0.50	1	Beach ridge	Albero and Angiolini (1983)	
	Ar	Estancia La Calera 5	33°15′0.00″	59°30′0.00″	AC-0416	5610	110	6250	6005	5743	*Erodona mactroides*	B	4.2		1	Beach ridge	Guida and González (1984); Albero and Angiolini (1985)	
	Ar	Estancia La Calera 6	33°15′0.00″	59°30′0.00″	AC-0417	5750	110	6375	6144	5906	*Erodona mactroides*	B	3.6		1	Beach ridge	Guida and González (1984); Albero and Angiolini (1985)	
22	Uy	C. Morgan 1	33°15′12.99″	58°21′5.92″	URU0114	5480	72	6011	5843	5649	*Erodona mactroides*	B	4.3	0.50	1	Beach ridge	Bracco and Ures (1998)	
	Uy	C. Morgan 2	33°15′12.99″	58°21′5.92″	URU0115	5520	72	6098	5894	5708	*Erodona mactroides*	B	4.3	0.50	1	Beach ridge	Boksar and Pantazi (1998)	
23	Uy	Nuevo Berlín	32°59′6.18″	58°3′38.98″	URU0177	5520	70	6093	5894	5711	*Erodona mactroides*	B	4.3	0.50	1	Beach ridge	Boksar and Pantazi (1998)	
24	Ar	Escuela N° 34 La Calera-Médanos	33°13′48.50″	59°25′16.22″	LP-1548	5510	90	6114	5881	5654	*Erodona mactroides* + *Mactra patagonica*	B	2	0.5	1	Estuarine	Amato and Silva Busso (2009); S. Amato (pers. com., 2015)	
	Ar	Escuela N° 34 La Calera-Médanos	33°13′48.50″	59°25′16.22″	LP-1590	7450	80	8080	7899	7712	*Erodona mactroides* + *Mactra patagonica*	B	0	0.5	1	Estuarine	Amato and Silva Busso (2009); S. Amato (pers. com., 2015)	
25	Uy	Villa Soriano 1	33°24′23.00″	58°19′32.00″	LP-744	5530	80	6128	5907	5703	*Erodona mactroides*	B	3.8		1	Parautochthonous shell concentrations in sand	Martínez et al. (2006); S. Martínez (pers. com., 2013)	H
	Uy	Villa Soriano 2	33°24′23.00″	58°19′32.00″	LP-740	5840	72	6409	6249	6063	*Erodona mactroides*	B	3.3		1	Parautochthonous shell concentrations in sand	Martínez et al. (2006); S. Martínez (pers. com., 2013)	I
	Uy	Villa Soriano 3	33°24′25.47″	58°19′21.65″	URU0072	5850	62.4	6399	6260	6115	*Erodona mactroides*	B	4.8		1	Beach	Boksar and Pantazi (1998)	
	Uy	Villa Soriano 4	33°24′25.47″	58°19′21.65″	URU0069	5910	62.4	6453	6321	6188	*Erodona mactroides*	B	4.8		1	Beach	Boksar and Pantazi (1998)	
26	Ar	Puesto Gómez	33°13′12.00″	59°31′12.00″	AC-0419	5620	110	6256	6016	5753	*Erodona mactroides*	B	4		1	Beach ridge	Guida and González (1984); Albero and Angiolini (1985)	
27	Ar	Entre Ríosa	33°16′12.00″	58°27′0.00″	AC-0422	5680	110	6312	6075	5834	*Erodona mactroides*	B	5		1	Beach ridge	Albero and Angiolini (1985)	

(*continued on next page*)

Table 1 (*continued*)

Sites	C.	Name	Latitude	Longitude	Lab. code	^{14}C age (yr BP)		Calibrated age range (cal. yr BP)			Material dated	Salinity	Elevation (m)		MSL error +/− (m)	Depositional environment	Reference	MA
						Age	Error +/−	Max	Median	min			MSL	Error +/−				
28	Ar	Puesto Pinasco	33°12′0.00″	59°31′48.00″	AC-0420	5680	110	6312	6075	5834	*Erodona mactroides*	B	3.15		1	Beach ridge	Guida and González (1984); Albero and Angiolini (1985)	
29	Ar	Entre Ríos	33°13′44.70″	59°30′24.00″	AC-1616	5690	170	6437	6080	5692	*Erodona mactroides*	Br	5		1	Beach ridge	Cavallotto et al. (2002)	
	Ar	Entre Ríos	33°13′41.50″	59°30′26.80″	UIC10497	5871	42	6384	6281	6188	*Erodona mactroides*	B	5		1	Beach ridge	Cavallotto et al. (2002)	
30	Uy	Arroyo Sauce de Nueva Palmira	33°50′32.00″	58°24′43.00″	AA88350	5714	64.3	6262	6113	5950	*Anomalocardia brasiliana*	O/B	3.8		1	Beach storm	Martínez and Rojas (2013)	
	Uy	Arroyo Sauce de Nueva Palmira	33°50′40.00″	58°24′42.00″	AA88351	5728	55.7	6265	6130	5981	*Anomalocardia brasiliana*	O/B	3.8		1	Beach storm	Martínez and Rojas (2013)	
31	Ar	Potrero Manantiales	33°13′48.00″	59°28′12.00″	AC-0421	5720	110	6347	6114	5881	*Erodona mactroides*	B	4.5		1	Beach ridge	Guida and González (1984); Albero and Angiolini (1985)	
32	Ar	Isla Martín García	34°10′52.17″	58°14′46.49″	AC-0431	5740	130	6417	6132	5859	*Erodona mactroides* + *Mactra isabelleana*	B	3.7		1	Estuarine	Albero and Angiolini (1985); González and Ravizza (1987)	J
	Ar	Isla Martín García	34°10′52.17″	58°14′46.49″	AC-0477	5800	120	6444	6199	5918	*Erodona mactroides* + *Mactra isabelleana*	B	3.7		1	Estuarine	Albero and Angiolini (1985); González and Ravizza (1987)	J
33	Ar	Entre Ríos	32°59′	58°30′	AC-0424	5820	110	6451	6222	5952	*Erodona mactroides*	B	2.3		1	Beach ridge	Albero and Angiolini (1985)	
34	Uy	Fray Bentos	33°6′52.75″	58°18′43.45″	URU0073	6000	60	6556	6406	6275	*Erodona mactroides*	B	3.5	0.25	1	Tidal flat	Boksar and Pantazi (1998)	
35	Ar	Manzanares	34°27′42.00″	58°59′6.00″	LP-185	6000	80	6612	6411	6258	*Erodona mactroides*	B	3.25	0.25	1	Estuarine	Figini (1992); E. Fucks (pers. com., 2013)	K
	Ar	Manzanares	34°27′42.00″	58°59′6.00″	LP-256	6200	90	6852	6631	6410	*Tagelus plebeius*	B	3.25	0.25	1	Estuarine	Figini (1992); E. Fucks (pers. com., 2013)	L
	Ar	Manzanares	34°27′42.00″	58°59′6.00″	LP-250	6370	90	7091	6835	6619	*Tagelus plebeius*	B	3.25	0.25	1	Estuarine	Figini (1992); E. Fucks (pers. com., 2013)	L
36	Ar	Punta Lara	34°52′07.00″	58°03′54.00″	LP-197	6020	90	6645	6434	6258	*Heleobia australis*	B	6.5		1	Beach ridge	Cavallotto et al. (2004); J.L. Cavallotto (pers. com., 2013)	
37	Uy	Solís Grande	34°45′35″	55°25′55″	UGAMS 11502	7160	30	7689	7619	7552	*Heleobia australis*	B	−5.50		1	Estuarine	Mourelle et al. (2015)	
38	Ar	Isla Talavera - Zárate	33°58′2.49″	58°57′57.53″	LP-1581	5980	70	6566	6387	6248	*Erodona mactroides* + *Mactra patagonica*	B	−14	0.5	1	Estuarine	Amato and Silva Busso (2009); S. Amato (pers. com., 2015)	
39	Ar	Escuela N° 11 El Cazador Escobar	34°17′52.09″	58°45′27.74″	LP-1589	7130	90	7774	7599	7430	*Erodona mactroides* + *Mactra patagonica*	B	−16	0.5	1	Estuarine	Amato and Silva Busso (2009); S. Amato (pers. com., 2015)	

Mollusc associated (MA) updated in terms of nomenclature.
A: *Erodona mactroides, Neocorbicula limosa, Heleobia piscium.*
B: *Erodona mactroides, Neocorbicula paranensi, Heleobia piscium.*
C: *Glycymeris longior, Mytilus edulis, Brachidontes darwinianus, Ostreola equestris, Plicatula gibbosa, Carditamera plata, Crassinella maldonadoensis, Mactra isabelleana, Clausinella gayi, Amiantis purpurata, Caryorbula caribaea, Corbula lyoni, Corbula* sp., *Lottia subrugosa, Diodora patagonica, Calliostoma juncudum, Echinolittorina lineolata, Heleobia australis, H. charruana,* Bostrycapulus aculeatus, *Marshallora nigrocincta, Seila adamsii, Epitonium albidum, Urosalpinx cala, Hanetia haneti, Costoanachis sertulariarum, Parvanachis paessleri, Olivella tehuelcha, Siphonaria lessoni,* Ellobiidae indet., Chiton species.
D: Chiton species.
E: *Mactra isabelleana, Heleobia australis.*
F: *Mactra* sp.
G: *Erodona mactroides, Buccinanops cochlidium, Olivancillaria carcellesi, O. urceus, Pitar rostratus, Ostrea puelchana, Noetia bisulcata.*
H: *Lunara ovalis, Ostreola equestris, Mactra isabelleana, Tagelus plebeius, Anamolocardia brasiliana, Pitar rostratus, Caryocorbula caribaea, Heleobia australis, H. charruana.*
I: *Ostrea* sp., *Mactra isabelleana, Tagelus plebeius, Anomalocardia brasiliana, Pitar rostratus, Caryocorbula caribaea, Corbula patagonica, Heleobia australis, H. charruana.*
J: *Brachidontes rodriguezii, Tagelus plebeius.*
K: *Tagelus plebeius.*
L: *Erodona mactroides.*

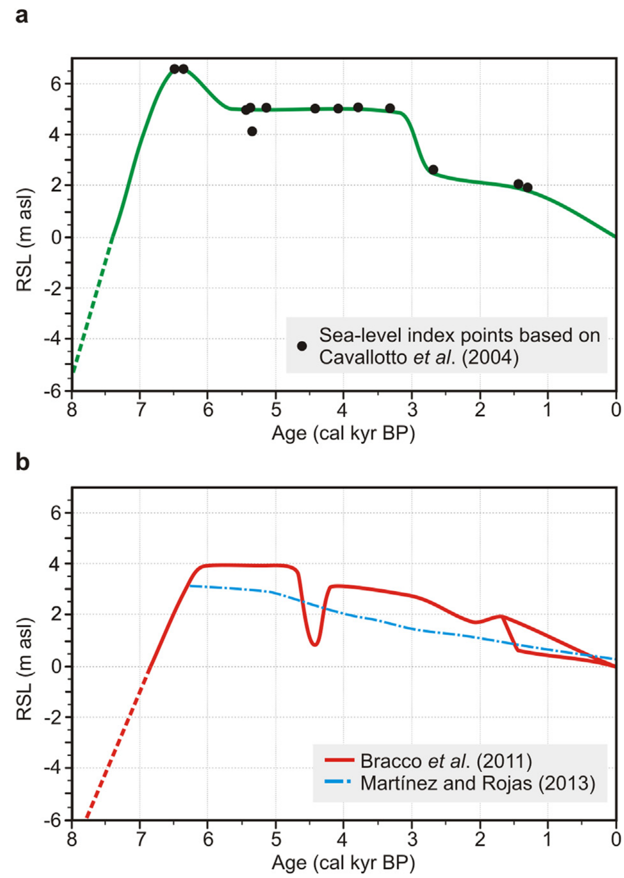

Fig. 2. Curves of relative sea-level variations for the past 8000 cal yr BP along the (a) southern Río de la Plata based on Cavallotto et al. (2004) redrawn by Gyllencreutz et al. (2010); (b) Uruguayan coast including data from the northeastern Río de la Plata and Atlantic coast modified from Bracco et al. (2011) and Martínez and Rojas (2013). Curves are plotted on the same age and elevation scale.

Data from the Argentine shelf listed in Guilderson et al. (2000) was considered to investigate the RSL at earlier times. Some of the data is from the latitude range 38.23° − 39.78°S which is within a few degrees of Buenos Aires Province. The material dated was from shell layers sampled by piston-coring in the late 1950s and early 1960s and stored at the Lamont Doherty Earth Observatory. The authors refer to Richards and Craig (1963) in claiming that the shell layers are of littoral or shallow neritic origin. However, when all the data supplied in the paper was considered, rather than that selected from their figures, it became clear that there is young material found at considerable depth. There is also material of similar age at a wide range of depths (Fig. 3). The material is from latitudes ranging from 36.8° − 54.1°S and longitudes 54.3° − 66.5°W but GIA predictions of the RSL do not vary a great deal over that area. The authors use a simple model of isostatic compensation to predict the difference between eustatic and actual RSL to be 45 m at Last Glacial Maximum. This prediction is important to the authors' interpretation of the data as representing RSL. However it would not be applicable on the shelf so close to the coastline where GIA effects are significant (Milne and Mitovica, 2008; Fig. 1). It is therefore clear that not all the material can be indicating the RSL of the time and none of the data was included in the set of 56 data employed for the purpose of the present analyses.

Each of the radiocarbon dates described here has been converted to calibrated years before present using the program Calib Rev. 7.0.2 (Stuiver et al., 2005), calibrated against the Marine13 and SHCal13 calibration curves (Reimer et al., 2013). Marine samples

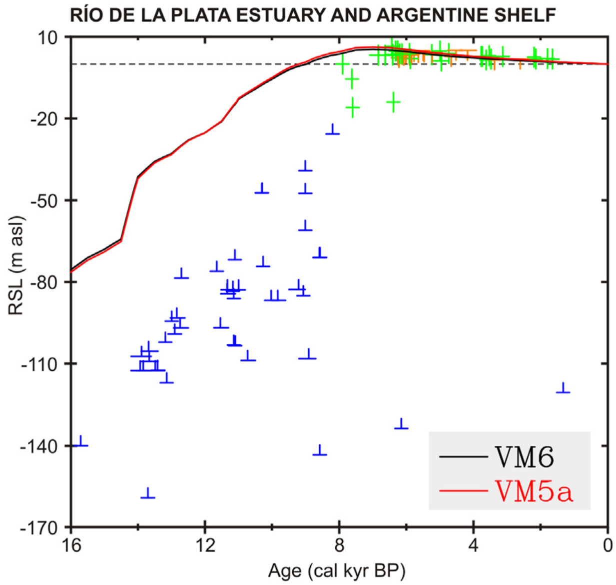

Fig. 3. Predicted relative sea-level for the ICE-6G_C model is shown for the last 16,000 cal yr BP together with all the data from the RDP (see Fig. 4 for details) and the Guilderson et al. (2000) data from the Argentine Shelf (in blue). (For interpretation of the references to colour in this figure legend, the reader is referred to the web version of this article.)

have been corrected for the 8 ± 17 year marine reservoir effect determined by Angulo et al. (2006). Dates are cited with a two sigma age range. We do not use the regional reservoir effect determined by Gómez et al. (2008) for the mollusks *Mactra isabelleana* and *Tagelus plebeius* because these data came for coastal locations southward of the RDP where a large ΔR was observed, which is explained by the input of content of dissolved carbonate by rivers and groundwater (the "hardwater effect"), an environmental situation that differs from that characteristic of the RDP.

E. mactroides and *Heleobia australis* are the most common molluscs found today in the middle fluvial zone (salinity 0.5–25‰) and fluvio-marine zone (salinity >25‰) of the RDP (Codignotto and Aguirre, 1993; Darrigran, 1994). *E. mactroides* and *M. isabelleana* are the dominant species in the unconsolidated bottom of the estuarial environment of the RDP (Scarabino et al., 2006).

To test the reasonableness of the hypothetical curve drawn by hand by Cavallotto et al. (2004) as a fit the RSL data, we have employed a high-degree polynomial regression analysis performed using the R language (R Core Team, 2013) and non-parametric regression using the program Past v.2.15 (Hammer et al., 2001). The selected biological samples come from workers using a relatively uniform methodology yielding comparable data, sufficiently robust for use in higher degree polynomial regression analysis. The results obtained from this analysis are employed in what follows to compare the resulting broad RSL reconstruction with GIA model predictions.

4. Results

Table 1 presents the individual entries of the database as estimated by the procedures detailed above and which were employed to produce the curves (Fig. 4). The subsurface data are scarce and only three have been chosen. One is situated near the RDP outlet on the Atlantic Ocean (site 37; Fig. 1, Table 1) dated at 7160 ± 30 ^{14}C yr BP (7940 cal yr BP) and the other two are from boreholes near the Paraná delta front (sites 38 and 39; Fig. 1, Table 1) dated at 5980 ± 70 ^{14}C yr BP (6387 cal yr BP) and 7130 ± 90 ^{14}C yr BP (7599 cal yr BP) respectively.

Additionally, data from the closest locations from the southern Argentine Shelf (37.23° – 39.78°S; Guilderson et al., 2000) were considered in discussion of the RSL curve for the last 16,000 cal yr BP.

It is important to note that all of the depositional environment information we present in Table 1 is based on the authors' descriptions in each paper employed in the compilation and do not imply any further interpretation. The radiocarbon data are mostly derived from shells recorded in coastal barrier, beach-ridges and storm beach deposits. Beach ridges and their associated deposits have been used to infer RSL changes. The altitudinal level of a beach ridge has been regarded as an approximate indicator of the past sea-level (Tamura, 2012) and the mean elevation of wave generated beach ridges is usually considered to be an approximate indicator of past maximum storm related sea-level (Otvos, 2000). However, some authors believe that some radiocarbon dates from beach ridges should be taken to imply short-term sea-level increases rather than the simple topographic expression of a storm deposit (Isla, 1998). Given the limitations to the data from this area, our analysis of RSL changes may be subjects to some bias.

4.1. Time–elevation plots of Holocene sea-level change

We regressed the elevation–time plots for 56 index points from our 39 sites on the RDP. We have included a current point at (0,0) in each regression to indicate present mean sea-level. Non-parametric "Loess" Smoothing (0.5 smooth), with 95% confidence interval based on 999 replicates obtained by resampling the residuals ("bootstrapping") was applied (Fig. 4b). A linear polynomial in the covariate was fitted to the data in the first instance, and the degree was increased by one until a decrease was noticed in the adjusted coefficient of determination R^2 (Table 1, Appendix A supplementary material). These low values are caused by the negative data that are badly fitted in the residual analysis (not shown). In a further step of the analysis the negative data (index points 37, 38 and 39) were excluded and a polynomial model with increasing degree (from linear to fifth-order) was fitted. The quartic polynomial was found to have best adjusted coefficient of determination R^2 of 0.472 (Table 1, Appendix A Supplementary material) so a polynomial of fourth degree was selected. Model diagnostic graphics demonstrated that the normality assumption is not reasonable as variance increases with the mean (Fig. 1 Supplementary material). Taking into account these results, a model with power variance function var = mean^p (Tweedie model) (Jorgensen, 1997) was chosen as an alternative statistical model. The optimum value for p was obtained for these data *via* profile likelihood, and it is close to a Gamma model. So a generalized linear model with gamma errors and canonical link was adjusted (Fig. 4c). Table 2 (Appendix A Supplementary material) shows coefficients and their standard errors, with the corresponding significance. All coefficients are highly significant. A deviation based R^2 measure was calculated and its value found to be 0.504, greater than one obtained for the normal model. Model diagnostic graphics are shown in Fig. 4c in which residuals are distributed at random around the y = 0.

The data is also shown in Fig. 4d in comparison with predicted curves from the GIA model ICE-6G_C (Peltier et al., 2015) using two different viscosity models VM5a and VM6 (Roy and Peltier, 2015).

5. Discussion

The smoothed curve from the Loess model suggests that RSL rose to reach the present level at ~7000 cal yr BP and the subsequent highstand occurred between 5800 and 5200 cal yr BP reaching as high as +4 m above present during a period of RSL stabilization between 6200 and 4900 cal yr BP with sea-level

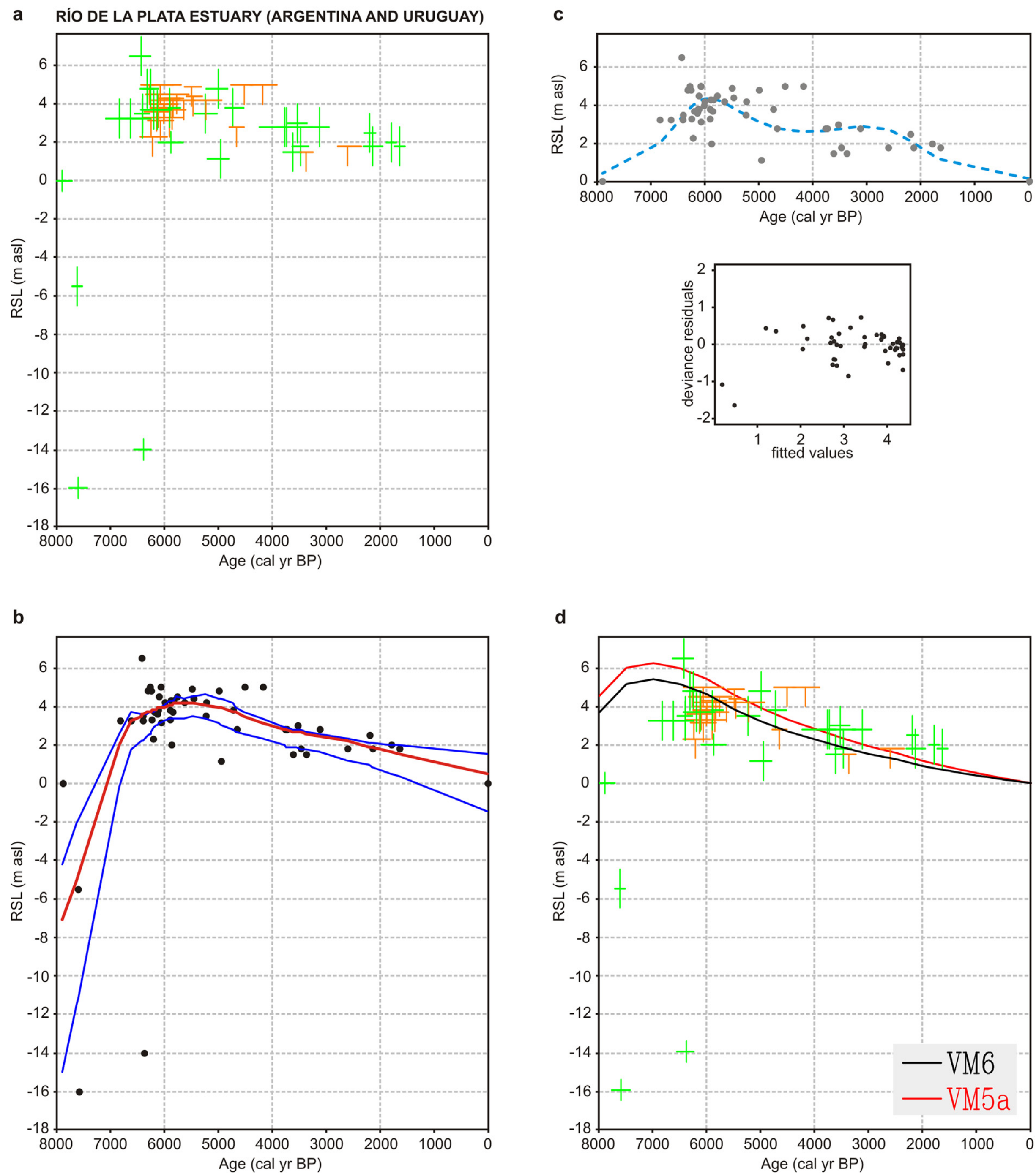

Fig. 4. (a) Relative sea-level reconstruction for the past 8000 cal yr BP from the Río de la Plata. Data from storm beaches and beach ridges is shown with a T-symbol, other data with + symbols. For sites locations see Fig. 1 and for details of each index point see Table 1. (b) Relative sea-level curve (envelope and smoothed) for the past 8000 cal yr BP obtained using a no-parametric "Loess" Smoothing. The red line represents the best-fitted sea-level curve and the blue lines represent the 95% confidence interval based on 999 replicates obtained by resampling the residuals ("bootstrapping"). The data outside the blue lines are index points outside the confidence interval. (c) Relative sea-level curve for the past 8000 cal yr BP obtained apply a generalized linear model with gamma errors and canonical link. (d) Predicted relative sea-level history for the past 8000 cal yr BP at RDP estuary for the ICE-6G_C model. Two curves are shown corresponding to predictions using the VM5a and VM6 viscosity models. (For interpretation of the references to colour in this figure legend, the reader is referred to the web version of this article.)

continuously declining thereafter towards the modern level (Fig. 4b). On the other hand, based on the Gamma model results an oscillating sea-level curve can be inferred with the Holocene highstand between 6300 and 5600 cal yr BP, again reaching up to +4 m above present at 6000 cal yr BP, followed by a ~1.5 m fall of sea-level which remained relatively stable until a rapid decrease after 2500 cal yr BP to its present position (Fig. 4c).

There is some disagreement on the timing and amplitude of the highstand and the period of stabilization which probably reflects differences in model parameterization and data precision. Neither the Gamma nor Loess model can claim statistical exclusivity with the data set. This allows for the possibility that there could been an oscillating curve following the highstand. It is important to take into account that the subsurface data are not included in the

Gamma model, which could be controlling the curve. The "smooth" model of late Holocene sea-level decline is, however, in close agreement with the GIA model predictions. While the altitudinal levels of beach ridges have been used as a rough indicator of past sea-level, they probably formed when the wave energy was sufficiently strong to rework the sediments above the medium sea-level in the inner RDP (Colombo et al., 2014) and therefore the heights proposed could be overestimated. Some inferences of neotectonic activity have been reported in the RDP area (e.g. Ríos et al., 1988; Parker, 1990; Codignotto et al., 1992; Guilderson et al., 2000). According to Colombo et al. (2014) if there was an isostatic uplift it is not considered to have influenced the formation of the attached beach ridges or cheniers in the last 6000 years. On the other hand, Cavallotto et al. (2004) believe that there is no conclusive evidence of neotectonic activity that would allow us to apply a reliable tectonic correction to the RSL curves. Moreover, a smooth decline over the past 6000 years would add further weight to the hydro-isostatic interpretation in the mid-to late Holocene in areas like RDP estuary unaffected by glacial isostasy or situated far from ("in the far-field of") the former ice sheets.

5.1. Comparison to geophysical model predictions

Comparison of the data with the RSL curves predicted by the ICE-6G_C GIA model (Figs. 3 and 4d), shows good agreement for the subaerial samples but not for the subsurface data. The subaerial data is telling a consistent story for the last 6000 years but the subsurface data are not in agreement with these data or with the GIA predictions. Since much of the subaerial data come from shells on beaches, beach ridges and storm beaches, they cannot be strictly interpreted as RSL index points. It seems likely that the predicted curves are somewhat high and the VM6 prediction is preferred over the prediction based upon use of viscosity model VM5a.

5.2. Comparison of RSL curves with the different geomorphological evolution models

According to Cavallotto and Violante (2005), the geomorphological evolution of the RDP is related to sea-level fluctuations and climate change after the LGT and the sedimentary sequence has been interpreted as a depositional sequence consisting of a transgressive system tract (TST) and a highstand system tract (HST) (Fig. 5). On the contrary, Richiano et al. (2012) and Colombo et al. (2014) interpreted that part of the TST deposits may correspond to the HST and the HST as a falling stage system tract (FSST) (Fig. 5). If the data from the Argentine Shelf is included, it suggests that sea-level rose incredibly fast between 16,000 and 8000 cal yr BP (Fig. 3). The present position was reached at or before c. 7000 cal yr BP (Fig. 4). As a consequence the transgression flooded the RDP paleovalley led primarily to the formation of an estuarine environment. As sea-level rose, a huge estuary occupied most of the RDP fluvial valley and most of the lower reaches of the streams that flow into the RDP (Cavallotto and Violante, 2005). This resulted in the extension of the former RDP estuary as far as the city of Diamante (Fig. 1), where the Paraná River mouth was located (Colombo et al., 2014). Transgressive events occurred in at least three stages of advance and retreat represented by an alternation of estuarine and marginal coastal environments (Amato and Silva Busso, 2009) (Fig. 5). At the same time, in adjacent coastal areas the shoreline retreated northwestward. In the study area, the base of the estuarine deposits overlies Plio-Pleistocene units, covers most of the RDP paleovalley and conforms to the contours of the substrate. The base of these deposits is located between −30 and 0 m, while the top is between −10 and 3 m, with a maximum thickness of 20 m (Cavallotto and Violante, 2005). Lack of extensive and high quality outcrops of deposits assigned to the TST and because these deposits are known mostly on the basis of drilling precludes the accurate determination of a continuous connection from a TST to a HST (Richiano et al., 2012). The evidence from this study suggests that the transgressive event continued until c. 6300–5800 cal yr BP. The RSL highstand (maximum Holocene sea-level) reached c. +4 m between 6300 and 5600 cal yr BP or between 5800 and 5200 cal yr BP (depending on the statistical method used) or at c. 7000 cal yr BP according to the ICE-6G model prediction. After this time the sea-level fell to the current position in a manner that is not precisely determinable (Fig. 5). According to Colombo et al. (2014), during the highstand shell accumulations along the estuarine coastal barrier developed in the inner RDP estuary (Fig. 1). A carcass of *Balaenoptera* cf. *physalus* was found at 33°48′S − 59°30′W near of city of Baradero, ~290 km north-westward of the RDP mouth (Fig. 1). Bone collagen was dated at 5540 ± 80 ^{14}C yr BP (6296 cal yr BP) (Fig. 5). The remains are associated with numerous shells of *Brachidontes rodriguezi* and *Mytilus platensis* in many cases complete and articulated and accompanied by a low proportion of *E. mactroides* and *H. australis* (Tonni et al., 1998) suggesting a mixohaline environment in a coastal plain.

After the highstand the FSST took place in two episodes (Amato and Silva Busso, 2009; Colombo et al., 2014) (Fig. 5). The first led to generation of the attached beach ridge sets (Fig. 1) during a gradual sea-level fall; the second episode represents an accelerated sea-level fall that resulted in the generation of cheniers, the south-eastwards avulsion of the Ibicuy River, the current Paraná delta, and in the transfer of the estuarine sedimentation to the area of the present coast (Colombo et al., 2014). The models provide no evidence to suggest that there has been a significant trend of change in the speed of sea-level fall during the FSST.

During the FSST beach ridges could developed as a consequence of a forced regression (FSST 1; Fig. 5) (Richiano et al., 2012) or during the late stage of sea-level rise (part of the HST) as previously interpreted by Cavallotto and Violante (2005) (Fig. 5). Coastal progradation became the most important process and a regressive sequence originated. Littoral areas similar to those found in the RDP region and southern Entre Ríos province were characterized by low energy prograding coasts with shelly and sandy beach ridges and cheniers as well as muddy tidal flats. At the time of generation of the beach ridges the discharge was probably similar to that occurring today and the Paraná River mouth was located near the city of Rosario, some 250 km further upstream (Iriondo, 2004) (Fig. 1). Our data suggest that the beach ridges formed during the regressive event between c. 5000 and 2000 cal yr BP, grading basinward to cheniers dated c. 1700 cal yr BP. According to Colombo et al. (2014) the preservation of the attached beach ridge sets could be a consequence of gradual RSL fall as predicted by the GIA model. The differences in height between the beach ridges could be related to fluctuations in RSL as suggested by one of the statistical methods. Another articulated carcass of *Eubalaena australis* was found in these attached beach ridge sets at Estancia El Palmar (33°27′33.11″S; 59°03′30.52″W; Fig. 1) 300 km to the northwest to the present RDP outlet carried by floatation to the inner RDP estuary by persistent winds and wind-driven currents and storm waves (Colombo et al., 2014).

According to Cavallotto (2002) and Cavallotto and Violante (2005) the Paraná delta began to form at c. 1800 cal yr BP. However, the oldest occupation of the Paraná delta for hunter–gatherer groups is dated at 2296 ± 34 ^{14}C yr BP (2233 cal yr BP) and 2267 ± 34 ^{14}C yr BP (2243 cal yr BP) (Loponte et al., 2012) (Figs. 1 and 5), suggesting that this delta area had already emerged before that time. The progradation of the coastal plains led to the current regional configuration and changed the previous estuarine environment to the current river conditions, characterized by the

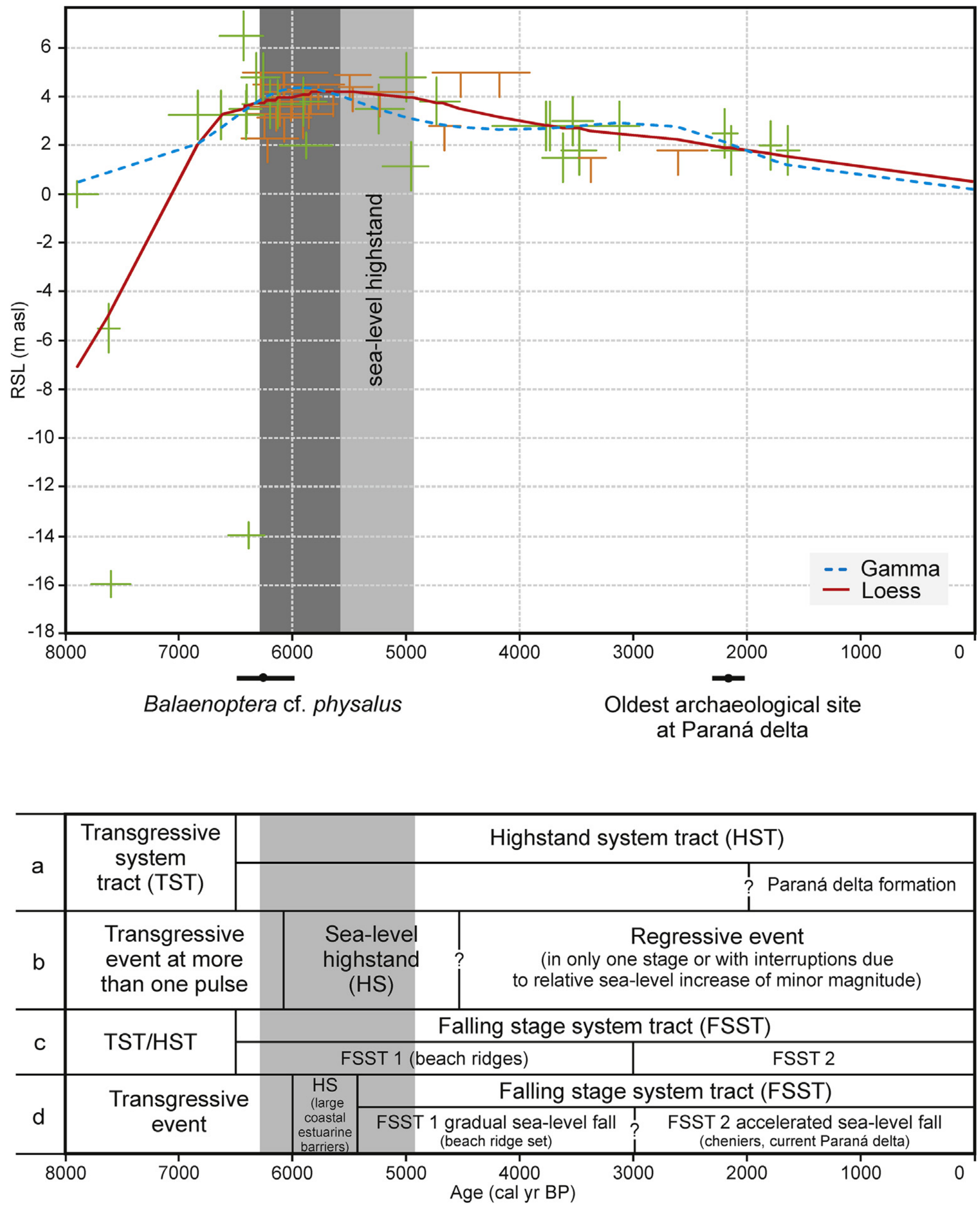

Fig. 5. Relative sea-level reconstruction for the past 8000 cal yr BP. The vertical shaded bar denote the period of RSL highstand proposed by using polynomial regressive analyses (see Fig. 4). Geomorphological evolution models according to a. Cavallotto and Violante (2005); b. Amato and Silva Busso (2009); c. Richiano et al. (2012) and d. Colombo et al. (2014).

delta development overlying the estuarine system. This change has been related to the progressive rapid advance of the Paraná delta to the south (Colombo et al., 2014).

5.3. Comparison the RSL curves with inferences about RSL based on palynological and diatomological data

Palynomorphs and diatoms changes from northern (Arroyo Solís Grande, Mourelle et al., 2015) and palynomorph changes from the southern coast (Río Salado, Vilanova and Prieto, 2012) of the RDP (Figs. 1 and 6) provided broad inferences concerning RSL history over the past c. 8000 cal yr BP. Salt-marsh sediments and their associated palynomorphs and diatoms are relatively good sea-level indicators during periods of rapid RSL rise (Murray-Wallace and Woodroffe, 2014). Salt-marsh plants that form distinctive elevation zones have the capability to reflect variations in tolerances to the frequency and duration of tidal inundations (Masson-Delmotte et al., 2013). At Arroyo Solís Grande, results indicated that sea-level reached the Holocene sea-level highstand between 6300 and 5100 cal yr BP indicated by highest and more stable acritarch values and a peak of dinocysts related to a stabilization of tidal regime and a higher marine input (Fig. 6). On the other hand, pollen records indicate that salt-marsh vegetation developed around the estuary between 8000 and 5100 cal yr BP, as the sea-level rose and reached the highstand. Brackish marshes around the estuary between 5100 and 2900 cal yr BP reflect the late Holocene sea-level fall and associated increased input of freshwater (*Myriophyllum* and *Ruppia*). Brackish marshes and shallow salt pond environments between 2900 and 1000 cal yr BP are most probably linked to the Paraná delta formation and a further sea-level fall. Present-day

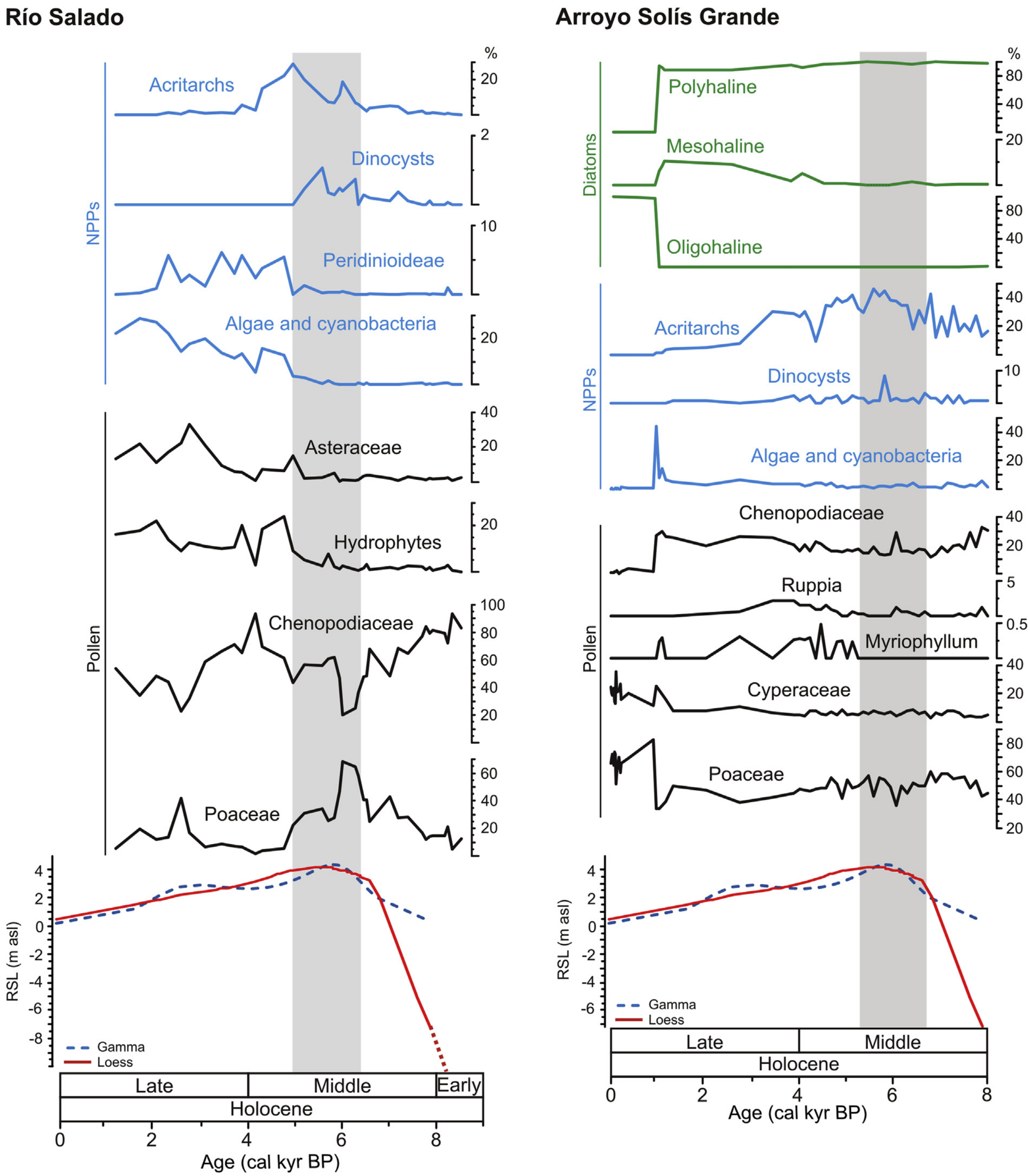

Fig. 6. Relative sea-level reconstruction from Río Salado and Arroyo Solís Grande using pollen, non-pollen palynomorphs (NPPs) and diatoms (adapted from Vilanova and Prieto, 2012, and Mourelle et al., 2015, respectively) and RSL curves from the Loess and Gamma models. Grey band represent the range of RSL highstand inferred by palynomorphs and diatoms.

marshes behind the sand bars characterized the last 1000 cal yr BP (Fig. 6).

At the southern margin of the RDP (Río Salado), low marsh brackish grasses and peaks of dinocysts suggest highest marine input and mixohaline conditions from c. 6200 to 5000 cal yr BP related to the sea-level highstand (Fig. 6) developed in an estuary which extended more than 25 km inland from the present coast and persisting c. 1000 years. From c. 8800 to 6200 cal yr BP a middle to high marsh prevailed with progressive tidal influence related to sea-level rise. This period is marked by low marsh with longer tidal submergence, higher inundation frequency, and higher energy in intertidal-subtidal estuarine environment. A transition from low marsh brackish grasses to a high marsh halophytic community occurred between c. 5000 and 4800 cal yr BP, followed by a transition to brackish marsh vegetation at c. 4800 cal yr BP with weaker estuarine conditions related to the regressive event. This reflects similar vegetation evolution on both RDP estuary coasts.

In the Río Salado the main change occurred between 5000 and 3100 cal yr BP as indicated by the increase of algae and cyanobacteria, Peridinoideae cysts and hidrophytes and disappearance of dinocysts. Specifically, from c. 3100 to 1080 cal yr BP environmental conditions were characterized by grasslands, co-dominating with halophytic vegetation (Chenopodiaceae) that gradually became dominant over the river floodplain and saline soils, and freshwater to brackish conditions without marine influence existed (Vilanova and Prieto, 2012). This is related to a wide paleo-Bahía Samborombón in which new beach ridges began to spread in decreasing levels toward the coast (Violante et al., 2001).

This interpretation of changing paleoenvironmental conditions is in good agreement with the RLS curves obtained by parametric and no-parametric methods. However, the small scale oscillations suggested by the Gamma model are not reflected by neither palynological nor diatom records. The current data set suggests a progressive decline of the RSL since the mid-Holocene highstand. The differences between the records seem to be related to the distance of the sampling site from the contemporaneous coastline.

6. Conclusions

The northeast region of Argentina and Uruguay along the east coast of the South American continent is a region far from former ice sheets (a “far-field site”) which is important in the study of RSL changes. The availability of a new paleo-sea-level data set for the RDP (Argentina and Uruguay) allowed us to analyze the Holocene RSL changes in this region and to capture thereby the general trend illustrated by the data which show good agreement with the ICE-6G_C (VM6) model. The substantial advantage of this data set is the significant improvement over that used in Cavallotto et al. (2004) and Martínez and Rojas (2013) for the same region. This improvement derives from the methodology used to arrange and compile the data set, the use of high-degree polynomial regression analyses and the comparison between the local predictions of sea-level history obtained with the VM6 model and geological inferences based upon sea-level indicators. Although the data compiled in the present study have their own uncertainties, a monotonic sea-level rise, a clear sea-level highstand and a progressive decline to the present position are predicted for the last 8000 years and the subaerial data tell a consistent story for the last 6000 years for the RDP. The “smooth” model of the late Holocene sea-level decline is in close agreement with both the GIA model predictions and the reconstruction of RSL from palynological and diatom records. The models provide no evidence to suggest that there has been a significant trend of change in the speed of sea-level fall during the FSST, as suggested by the different geomorphological evolution models. The Loess model, the GIA predictions and the trend inferred by palynological and diatom data trace out a slow sea-level fall for the last c. 6000 cal yr BP. Our results are in agreement with the trends of the mid- and late-Holocene RSL curve for Southern Brazil (Angulo et al., 2006) and the Uruguayan coast (Martínez and Rojas, 2013). However, the RSL curve from the RDP should not be seen as representative of the whole of both the Buenos Aires Province and Uruguay, because of differences between the estuary and the coastline which could have likely been differentially affected by hydro-isostasy/tidal range through the Holocene. We critically assessed published Holocene sea-level data from the RDP in order to produce a Holocene RSL curve of sufficient quality to provide a location in this area for testing theoretical models. Previous work for the Atlantic coast of South America by Milne et al. (2005) had a gap of approximately 24° in latitude between the locations in Santa Catarina, Brazil and Punta Arenas in the Strait of Magellan. The Argentine Shelf data published by Guilderson et al. (2000) was not included in Milne et al. (2005) and we also conclude that the uncertainties in its interpretation preclude its use in determining the RSL curve at more southerly locations.

Acknowledgements

Funding was provided by CONICET (Grant PIP 543), Universidad Nacional de Mar del Plata (Grant Exa 695/14) and FONCyT (Grant PICT 0950/14) to A.R.P. and NSERC Discovery Grant A9627 to W.R.P. and R.D. We are indebted to J. L. Cavallotto, S. Martínez, S. Amato, E. Fucks and the Laboratorio de Análisis de Tritio y Radiocarbono (LATyR) (La Plata, Argentina) for our continuing interactions regarding their carefully quality-controlled data bases for RSL history. To C. de Francesco for assistance to adapt the taxonomic status of molluscs. We are grateful to J.L. Cavallotto and an anonymous referee for their constructive comments.

Appendix A. Supplementary material

Supplementary material related to this article can be found at http://dx.doi.org/10.1016/j.quaint.2016.02.044.

References

Acha, E.M., Mianzan, H., Guerrero, R., Carreto, J., Giberto, D., Montoya, N., Carignan, M., 2008. An overview of physical and ecological processes in the Río de la Plata Estuary. Continental Shelf Research 28, 1579–1588.
Aguirre, M.L., Whatley, R.C., 1995. Late Quaternary marginal marine deposits and paleoenvironments from northeastern Buenos Aires Province, Argentina: a review. Quaternary Science Reviews 14, 223–254.
Albero, M.C., Angiolini, F.E., 1983. INGEIS radiocarbon laboratory dates I. Radiocarbon 25, 831–842.
Albero, M.C., Angiolini, F.E., 1985. INGEIS radiocarbon laboratory dates II. Radiocarbon 27, 314–337.
Amato, S., Silva Busso, A., 2009. Estratigrafía cuaternaria del subsuelo de la cuenca inferior del Río Paraná. Revista de la Asociación Geológica Argentina 64 (4), 594–602.
Angulo, R.J., Lessa, G.C., Souza, M.C., 2006. A critical review of mid- to Late-Holocene sea-level fluctuations on the eastern Brazilian coastline. Quaternary Science Reviews 25, 486–506.
Boksar, R.B., Pantazi, M.C.U., 1998. Las variaciones del nivel del mar y el desarrollo de las culturas prehistóricas del Uruguay. Revista do Museu de Arqueologia e Etnologia 8, 109–115 (São Paulo).
Bracco, R., Ures, C., 1998. Las variaciones del nivel del mar y el desarrollo de las culturas prehistóricas del Uruguay. Revista do Museu de Arqueologia e Etnologia 8, 109–115.
Bracco, R., García-Rodríguez, F., Inda, H., Del Puerto, L., Castiñeira, C., Panario, D., 2011. Niveles relativos del mar durante el Pleistoceno final-Holoceno en la costa de Uruguay. In: García-Rodríguez, F. (Ed.), El Holoceno en la zona costera de Uruguay. Departamento Publicaciones Udelar, Montevideo, pp. 65–92.
Bracco, R., Inda, H., Del Puerto, L., Capdepont, I., Panario, D., Castiñeira, C., García-Rodríguez, F., 2014. A reply to “Relative Sea level during the Holocene in Uruguay”. Palaeogeography Palaeoclimatology Palaeoecology 401, 166–170.
Cavallotto, J.L., 2002. Evolución holocena de la llanura costera del margen sur del Río de la Plata. Revista Asociación Geológica Argentina 57 (4), 376–388.
Cavallotto, J.L., Violante, R.A., 2005. Geología y Geomorfología del Río de la Plata. In: de Berrío, R.E., Etcheverry, M.F., Caballé, M.F., Llambias, E. (Eds.), Geología y Recursos Minerales de la Provincia de Buenos Aires. La Plata. XVI Congreso Geológico Argentino, Relatorio, pp. 237–254.
Cavallotto, J.L., Parker, G., Violante, R.A., 1995. Relative sea level changes in the Río de la Plata during the Holocene. In: Ortlieb, L. (Ed.), Late Quaternary Coastal Records of Rapid Change: Application to Present and Future Conditions. 2nd Annual Meeting. Abstracts. Antofagasta, Chile, pp. 19–20.
Cavallotto, J.L., Violante, R.A., Parker, G., 1999. Historia evolutiva del Río de la Plata durante el Holoceno. In: XIV Congreso Geológico Argentino, Salta. Actas, vol. 1, pp. 508–511.
Cavallotto, J.L., Colombo, F., Violante, R.A., 2002. Evolución reciente de la llanura costera de Entre Ríos. In: XV Congreso Geológico Argentino Actas, pp. 500–505 (El Calafate).
Cavallotto, J.L., Violante, R.A., Parker, G., 2004. Sea-level fluctuations during the last 8600 years in the de la Plata river (Argentina). Quaternary International 114, 155–165.
Cavallotto, J.L., Violante, R.A., Colombo, F., 2005. Evolución y cambios ambientales en la llanuera costera de la cabecera del río de la Pata. Revista de la Asociación Geológica Argentina 60, 353–367.
Codignotto, J.O., Aguirre, M.L., 1993. Coastal evolution, changes in sea level and molluscan fauna in northeastern Argentina during the Late Quaternary. Marine Geology 110, 163–175.

Codignotto, J.O., Kokot, R.R., Marcomini, S.C., 1992. Neotectonism and sea-level changes in the coastal zone of Argentina. Journal of Coastal Research 8 (11), 125–133.
Colado, U.R., Figini, A.J., Fidalgo, F., Fucks, E.E., 1995. Los depósitos marinos del Cenozoico Superior aflorantes en la zona comprendida entre Punta Indio y el Río Samborombón, Provincia de Buenos Aires. In: IV Jornadas Geológicas y Geofísicas Bonaerenses Actas, vol. I, pp. 151–158 (Junín).
Colombo, F., Serra, J., Rivero, L., 2014. Río de la Plata inner estuary (Argentina): main forms, sedimentary infill and Holocene evolution. In: Martini, I.P., Wanless, H.R. (Eds.), Sedimentary Coastal Zones from High to Low Latitudes: Similarities and Differences. Geological Society. Special Publication, London, p. 388.
Cortelezzi, C.R., Pavlicevic, R.E., Pittori, C.A., Parodi, A.V., 1992. Variaciones del nivel del mar en el Holoceno de los alrededores de La Plata y Berisso. In: Cuarta Reunión Argentina de Sedimentología, pp. 131–138 (La Plata).
Darrigran, G.A., 1994. Composición de la malacofauna litoral del estuario del Río de la Plata. República Argentina. In: I Congreso and III Reunión Argentina de Limnología. Tankay, vol. I, pp. 147–149.
D'Onofrio, E.E., Fiore, M.M.E., Pousa, J.L., 2008. Changes in the regime of storm surges at Buenos Aires, Argentina. Journal Coastal Research 24, 260–265.
Figini, A.J., 1992. Edades ^{14}C de sedimentos marinos holocénicos de la Provincia de Buenos Aires. In: 3° Jornadas Geológicas Bonaerenses Actas, pp. 147–152 (La Plata).
Fucks, E.E., Blasi, A.M., Carbonari, J., Huarte, R., Pisano, F., Aguirre, M.L., 2011. Evolución geológica-geomorfológica de la cuenca del Río Areco, NE de la Provincia de Buenos Aires. Revista de la Asociación Geológica Argentina 68, 109–120.
Fucks, E.E., De Francesco, F.O., 2003. Ingresiones marinas al norte de la ciudad de Buenos Aires; su ordenamiento estratigráfico. In: Actas II Congreso Argentino de Cuaternario y Geomorfología, pp. 101–110 (Tucumán).
Gómez, E.A., Perillo, G.M.E., 1995. Submarine outcrops underneath shoreface-connected sand ridges, outer Bahía Blanca Estuary, Argentina. Quaternary of South America & Antarctic Peninsula 9, 23–37 (Rotterdam, Balkema Publishers).
Gómez, E.A., Martínez, D.E., Borel, C.M., Guerstein, G.R., Cusminsky, G.C., 2006. Negative sea level oscillation in Bahía Blanca estuary related to a global climatic change around 2650 yr BP. Journal of Coastal Research Special Issue 39, 181–185.
Gómez, E.A., Borel, C.M., Aguirre, M.L., Martínez, D.E., 2008. Radiocarbon reservoir ages and hardwater effect for the northeastern coastal waters of Argentina. Radiocarbon 50 (1), 119–129.
González, M.A., Ravizza, G., 1987. Sedimentos estuáricos del Pleistoceno tardío y Holoceno en la Isla Martín García, Río de la Plata. Asociación Geológica Argentina 42, 231–243.
Guida, N.G., González, M.A., 1984. Evidencias paleoestuáricas en el sudeste de Entre Ríos, su evolución con niveles marinos relativamente elevados del Pleistoceno Superior y Holoceno. In: Noveno Congreso Geológico Argentino, 577–594. San Carlos de Bariloche.
Guilderson, T.P., Burckle, L., Hemming, S., Peltier, W.R., 2000. Late Pleistocene sea level variations derived from the Argentine Shelf. Geochemistry Geophysics Geosystems. An electronic journal of the Earth Sciences 1.
Gyllencreutz, R., Mahiques, M.M., Alves, D.V.P., Wainer, I.K.C., 2010. Mid- to late-Holocene paleoceanographic changes on the southeastern Brazilian shelf based on grain size records. The Holocene 20 (6), 863–875.
Hammer, Ø., Harper, D.A.T., Ryan, P.D., 2001. PAST: Paleontological statistics software package for education and data analysis. Palaeontologia Electronica 4, 9.
Iriondo, M., 2004. The littoral complex at the Paraná mouth. Quaternary International 114, 143–154.
Isla, F.I., 1989. The Southern Hemisphere sea-level fluctuations. Quaternary Science Reviews 8, 359–368.
Isla, F.I., 1998. Holocene coastal evolution in Buenos Aires Province, Argentina. Quaternary of South America and Antarctic Peninsula 16, 297–321 (A.A. Balkema. Rotterdam).
Isla, F.I., Espinosa, M.A., 1998. Modelo sedimentario de colmatación de pequeños estuarios dominados por limo, Provincia de Buenos Aires. In: VII Reunión Argentina de Sedimentología, Actas, pp. 24–36 (Salta).
Jorgensen, B., 1997. The Theory of Dispersion Models. Chapman and Hall.
Loponte, D., Acosta, A., Mucciolo, L., 2012. Contribución a la arqueología del Delta del Paraná: El nivel acerámico del sitio Isla Lechiguanas 1. Comechingonia. Revista de Arqueología 16, 229–268 (Córdoba).
Martínez, S., Rojas, A., 2013. Relative sea level during the Holocene in Uruguay. Palaeogeography Palaeoclimatology Palaeoecology 374, 123–131.
Martínez, S., Rojas, A., 2014. Comments to A reply to Relative sea level during the Holocene in Uruguay' by Bracco et al. (2013). Palaeogeography Palaeoclimatology Palaeoecology 401, 171–172.
Martínez, S., Rojas, A., Ubilla, M., Verde, M., Perea, D., Piñeiro, G., 2006. Molluscan assemblages from the marine Holocene of Uruguay: composition, geochronology, and paleoenvironmental signals. Ameghiniana 43, 385–398.
Masson-Delmotte, V., Schulz, M., Abe-Ouchi, A., Beer, J., Ganopolski, A., González Rouco, J.F., Jansen, E., Lambeck, K., Luterbacher, J., Naish, T., Osborn, T., Otto-Bliesner, B., Quinn, T., Ramesh, R., Rojas, M., Shao, X., Timmermann, A., 2013. Information from paleoclimate archives. In: Stocker, T.F., Qin, D., Plattner, G.-K., Tignor, M., Allen, S.K., Boschung, J., Nauels, A., Xia, Y., Bex, V., Midgley, P.M. (Eds.), Climate Change 2013: the Physical Science Basis. Contribution of Working Group I to the Fifth Assessment Report of the Intergovernmental Panel on Climate Change Cambridge University Press, Cambridge, United Kingdom and New York, NY, USA.
Milne, G.A., Mitovica, J.X., 2008. Searching for eustasy in deglacial sea-level histories. Quaternary Science Reviews 27, 2292–2302. http://dx.doi.org/10.1016/j.quascirev.2008.08.018.
Milne, G.A., Long, A.J., Bassett, S.E., 2005. Modelling Holocene relative sea-level observations from the Caribbean and south America. Quaternary Science Reviews 24, 1183–1202.
Mourelle, D., Prieto, A.R., Pérez, L., García-Rodríguez, F., Borel, C.M., 2015. Mid and late Holocene multiproxy analysis of environmental changes linked to sea-level fluctuation and climate variability of the Río de la Plata estuary. Palaeogeography, Palaeoclimatology, Palaeoecoleogy 421, 75–88.
MTOP, 1980. Conservación y mejora de playas – URU. 73.007. In: Ministerio de Transporte y Obras Públicas. Programa de las Naciones Unidas para el Desarrollo – UNESCO, Uruguay (Informe Técnico).
Murray-Wallace, C.V., Woodroffe, C.D., 2014. Quaternary Sea-level Changes: a Global Perspective. Cambridge University Press, New York, 484 pp.
Otvos, E.G., 2000. Beach ridges-definitions and significance. Geomorphology 32, 83–108.
Parker, G., 1990. Estratigrafía del Río de la Plata. Revista de la Asociación Geológica Argentina 45 (3–4), 193–204.
Peltier, W.R., Argus, D.F., Drummond, R., 2015. Space geodesy constrains ice age terminal deglaciation: the global ICE-6G_C (VM5a) model. Journal of Geophysic Research Solid Earth 120, 450–487. http://dx.doi.org/10.1002/2014JB011176.
Pousa, J.L., D'Onofrio, E.E., Fiore, M.M.E., Kruse, E.E., 2013. Environmental impacts and simultaneity of positive and negative storm surge on the coast of the Province of Buenos Aires, Argentina. Environmental Earth Science 68, 2325–2335.
R Core Team, 2013. R: a Language and Environment for Statistical Computing. R Foundation for Statistical Computing, Vienna, Austria. http://www.R-project.org/.
Reimer, P.J., Bard, E., Bayliss, A., Beck, J.W., Blackwell, P.G., Ramsey, C.B., Buck, C.E., Cheng, H., Edwards, R.L., Friedrich, M., Grootes, P.M., Guilderson, T.P., Haflidason, H., Hajdas, I., Hatte, C., Heaton, T.J., Hoffmann, D.L., Hogg, A.G., Hughen, K.A., Kaiser, K.F., Kromer, B., Manning, S.W., Niu, M., Reimer, R.W., Richards, D.A., Scott, E.M., Southon, J.R., Staff, R.A., Turney, C.S.M., Van der Plicht, J., 2013. IntCal13 and Marine13 radiocarbon age calibration curves 0–50,000 years cal BP. Radiocarbon 55, 1869–1887.
Richards, H.G., Craig, R., 1963. Pleistocene sedimentation and fauna of the Argentine Shelf, II, Pleistocene molluscs from the continental shelf off Argentina. Proceeding of Academic of Natural Science, Philadelphia 115, 127–152.
Richiano, S., Varela, A.N., D'Elia, L., Bilmes, A., Aguirre, M., 2012. Evolución paleoambiental de cordones litorales holocenos durante una caída del nivel del mar en la Bahía Samborombón, Buenos Aires, Argentina. Latin American journal of sedimentology and basin analysis 19 (2), 105–124.
Ríos, F.F., Gianibelli, J.C., Barrio, L., 1988. Aspectos geonómicos de los bordes continentales costeros del aulacógeno del Salado, Provincia de Buenos Aires. In: II Jornadas Geológicas Bonaerenses, Bahía Blanca, Actas, pp. 489–498.
Rojas, A., 2002. Tafonomía y cronología de nuevos depósitos fosilíferos del Holoceno marino de Uruguay. In: II Jornadas uruguayas del Cenozoico. Montevideo, pp. 80–82.
Rojas, A., Urteaga, D., 2011. Late Pleistocene and Holocene chitons (Mollusca, Polyplacophora) from Uruguay: Palaeobiogeography and palaeoenvironmental reconstruction in mid-latitudes of the southwestern Atlantic. Geobios 44, 377–386.
Rostami, K., Peltier, W.R., Mangini, A., 2000. Quaternary marine terraces, sea-level changes and uplift history of Patagonia, Argentina: comparisons with predictions of the ICE-4G (VM2) model of the global process of glacial isostatic adjustment. Quaternary Science Reviews 19, 1495–1525.
Roy, K., Peltier, W.R., 2015. Glacial isostatic adjustment, relative sea level history and mantle viscosity: reconciling relative sea level model predictions for the U.S. East coast with geological constraints. Geophysical Journal International 201, 1156–1181.
Scarabino, F., Zaffaroni, J.C., Clavijo, C., Carranza, A., Nin, M., 2006. Bivalvos marinos y estuarinos de la costa uruguaya: faunística, distribución, taxonomía y conservación. In: Menafra, R., Rodríguez-Gallego, L., Scarabino, F., Conde, D. (Eds.), Bases para la conservación y el manejo de la costa uruguaya. Vida Silvestre, Montevideo, pp. 157–169.
Sepúlveda, H.H., Valle-Levinson, A., Framiñan, M.B., 2004. Observations of subtidal and tidal flow in the Río de laP lata Estuary. Continental Shelf Research 24, 509–525.
Servicio de Hidrografía Naval, 1999. Derrotero Argentino, Parte I, Río de la Plata. Armada Argentina, H-201, Buenos Aires, Argentina, 296 p.
SIRGAS Project, 1997. Sistema de Referncia Geocêntrico para a América do Sul, SIRGAS Project Final Report. International Association of Geodesy Scientific Assembly, Río de Janeiro, 99 pp.

Stuiver, M., Reimer, P.J., Reimer, R.W., 2005. CALIB 5.0 (WWW Program and Documentation).
Tamura, T., 2012. Beach ridges and prograded beach deposits as palaeoenvironment records. Earth-Science Reviews 114, 279–297.
Tonni, E.P., Cione, A.L., Figini, A.J., 1998. Calibración de edades radiocarbono y condiciones de salinidad en la ingresión del Holoceno temprano en el noreste de la provincia de Buenos Aires. In: VII Congreso Argentino de Paleontología y Bioestratigrafía, Bahía Blanca.
Vilanova, I., Prieto, A.R., 2012. Historia de la vegetación de las llanuras costeras de la Bahía Samborombón (~35,5°S), Argentina, desde 7800 ^{14}C años. Ameghiniana 49, 303–318.
Violante, R.A., Parker, G., Cavallotto, J.L., 2001. Evolución de las llanuras costeras del este bonaerense entre la bahía Samborombón y la laguna Mar Chiquita durante el Holoceno. Revista de la Asociación Geológica Argentina 56, 51–66.